Recrystallization Kinetics of the ECAP processed stainless steel 316L

A. Abooie Mehrizi[1], M. H. Farshidi*[2]

Department of Materials Science and Metallurgical Engineering, Ferdowsi University of Mashhad, Mashhad, Iran

Abstract

Austenitic stainless steels are widely used in different industries because of their attractive mechanical properties and good corrosion resistance. While different works have been focused on the severe plastic deformation of austenitic stainless steels, recrystallization kinetics of these alloys after the imposition of severe plastic deformation has remained less studied. The aim of this work is to study the recrystallization kinetics of austenitic stainless steel 316L after the imposition of severe plastic deformation using equal channel angular pressing. For this purpose, the alloy is processed by UnECAPed, 1, 2, and 4 passes of the mentioned process at 310 ºC by route BC. Afterward, the processed specimens are subjected to annealing at 800 ºC for 9 to 30 min. During this procedure, the kinetics of recrystallization is studied using optical microscopy while the optical microscopy results are analyzed by the MIP5 image analyzing software. Also, the volume fraction of recrystallization is interpreted using the JMAK model. Results show that the volume fraction of recrystallization for 2 and 4 pass specimens completed in 30 min. and equiaxed microstructure with a grain size less than 10μm can be obtained. The exponent of recrystallization duration in the JMAK model is between 3 and 4. This indicates the three-dimensional growth of the recrystallized grains and the decrease in the nucleation rate of the grains. The mechanism probably involving these phenomena is discussed.

Keywords: Severe plastic deformation, Annealing, Stainless steel 316L, Grain size, Recrystallization kinetics.

1. Introduction

One of the important issues in material science and engineering is the improvement of the mechanical properties of metallic material. Grain refinement of metallic materials is one of the main approaches to increase of their strength. One of methods applied for grain refinement of metallic materials is the imposition of severe plastic deformation (SPD) and therefore, different processes have introduced for the imposition of SPD [1]. Among these processes, equal channel angular pressing (ECAP) is widely applied because of its simplicity, its capability to impose a homogenous strain and its capability to impose variable strain paths [1]. In this process, the rod is passed through a die which has an angled channel similar to what is shown in Fig. 1. As a result of this process, a considerable shear strain is imposed on the material. Different parameters such as the die angle, number of the passes, and the process temperature affect the microstructures evolution and the mechanical properties of the materials during ECAP processing [1,2]. For example, reducing the die angles (φ *and* ψ), increasing the number of passes, and decreasing the processing temperature cause more rapid grain refinement of the materials through the ECAP processing. Also, the imposed strain path can be controlled by the process route. For instance, three different routes can be applied in the ECAP process. In route A, the rod is passed repetitively without any rotation. In the route B_C, the rod is rotated by the angle of 90between each pass in a constant direction. In the route C, the rod is rotated by 180° between passes. It is notable that the shape of a hypothetical square ele-

**Corresponding author*
farshidi@um.ac.ir
Address: Department of Materials Science and Metallurgical Engineering, Ferdowsi University of Mashhad, Mashhad, Iran.
1. M.Sc.
2. Assistant Professor

ment becomes similar to its initial state after two passes of route C and four passes of route B_C [3].

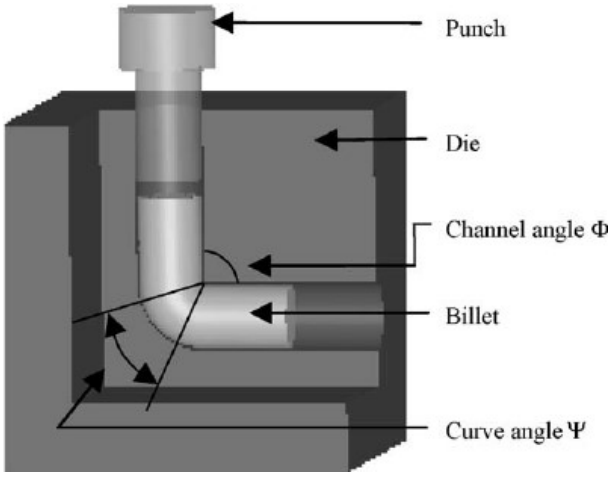

Fig. 1. Schematic illustration of the ECAP process for the cylindrical specimens [1].

Austenitic stainless steels (ASS) are attractive materials because of their corrosion resistance and biocompatibility. In these steels, Cr and Ni are two essential alloying elements, which improve the corrosion resistance of these materials [4]. However, the strength of these alloys is relatively low, and therefore, different works have focused on SPD processing of these alloys. The reason for this issue is high strain imposed on a bulk solid without the introduction of any significant change in the overall dimensions of the solid and leading to the production of exceptional grain refinement. For instance, Dubatkin et al. [5] have processed the ASS 316L by the ECAP process for up to 4 passes at room temperature. Their results have shown that the grain size of this alloy reached about 200 nm while the yield strength increased to 1500 MPa. The elongation reached from 90% in the initial state to 11% after the ECAP process. It is also reported that the grain size of 500 nm and yield strength of 870 MPa is obtained by ECAP processing at 400 C. the elongation was reduced to 25% [6]. It is also notable that the microstructure evolutions of ASS during SPD are affected by the processing temperature and their relatively low stacking fault energy (SFE). For more explanations, it is reported that the austenite phase of the ASS transforms to martensite during SPD at the cold deformation regime [7,8]. Despite this, when the SPD is performed at a warm deformation regime, the transformation of austenite to martensite is negligible [9]. Also, the twining deformation mechanism plays an extensive role during the SPD of ASS because of their low SFE, which slows the activity of dislocation glide [10,11].

Since SPD processing of ASS decreases their ductility and toughness, these materials are often subjected to post-SPD annealing. This annealing treatment results in the occurrence of discontinuous static recrystallization (DSRX) because of the relatively low SFE of ASS [12]. For instance, it is reported that the annealing treatment of the ECAP processed ASS 316L at 550℃ for 20h causes a partial DSRX, whereas the recrystallized grains having a diameter of 10-15μm appeared [13]. Although the mechanical properties variation and the microstructure evolutions during annealing of SPD processed ASS have been investigated to some extent [5,12,14] the kinetics of DSRX and the grain growth have been less studied. For example, it is reported that during annealing of the ECAP processed ASS 316L at temperatures under 700 ℃, the recrystallization rate is very slow. Nevertheless, the recrystallization rate is accelerated at the annealing temperature temperatures above 700 ℃ [1]. However, no comprehensive study has considered the quantifying models for DSRX of ASS subjected to SPD.

Multiple research have been devoted to quantifing the kinetic of DSRX considering different parameters like the spent annealing time, the applied temperature, and the imposed plastic strain. Johnson, Mehl, Avrami, and Kolmogorov (JMAK) have presented a well-known model [14] that is widely accepted to estimate the volume fraction of recrystallization considering different affecting parameters. This equation considers the random nucleation and growth of the recrystallized grains, and it relates the volume fraction of recrystallizing (X_V) to affecting parameters as follows:

$$X_V = 1 - \exp(-Bt^n) \quad \text{Eq.(1)}$$

Where t is the duration of recrystallization and B is a factor related to different parameters as below:

$$B = \frac{1}{4} f \dot{N} S^m \quad \text{Eq.(2)}$$

Here, $\dot{N}$ is the rate of nucleation per time or the number of stable nuclei that appeared at the initiation of the recrystallization, S is the speed of grain boundary migration, and f is a shape factor, while m is the number of growth directions of the nucleus. In the JMAK equation, the exponent of the time (n-value) is related to two different parameters: nucleation status and m. For instance, when nucleation is continued during the time of recrystallization, the n-value is equal to $m+1$ while $\dot{N}$ would be the nucleation rate per time. If the nucleation is only considered at the initiation of recrystallization, the n-value is equal to m, while would be the number of stable nuclei that appeared at the initiation of the recrystallization. Also, the recrystallization rate could be measured considering the time required for recrystallization of 50% of the microstructure ($t_{0.5}$), as follows: [14].

$$\text{Recrystallization rate} = 1/t_{0.5} \quad \text{Eq.(3)}$$

The aim of this work is to investigate the effect of ECAP processing combined with subsequent annealing treatments on the kinetic of DSRX of ASS 316L. For this purpose, microstructures of the processed materials are studied using optical microscopy, while the kinetics of

recrystallization and the growth of recrystallized grains are investigated using the JMAK and BT equations, respectively.

2. Materials and methods

ASS 316L cylindrical rods with a diameter of 10 mm are received and cut into 70 mm pieces. The chemical composition of the received material is shown in Table 1. The specimens were annealed at 1100°C for 2h and then quenched in water. The specimens were ECAP processed through route B_C for up to four passes. Then ECAP process was performed using a die with a channel angle of 90 at a temperature of 310±30 ℃. The effective plastic strain imposed onto a billet per pass for a given die geometry equals 1.15. More details about the ECAP processing are presented elsewhere [15].

The annealing treatment of ECAP processed specimens was performed at 800°C for different durations of 9 to 30 min. Then, the specimens are cut along their longitudinal axis, mechanically polished, and etched using HNO3-50%HCL as the chemical etchant. Microstructural observations were achieved using optical (OM) and scanning electron microscopes (SEM). MIP5 software was used to calculate the volume fraction and the grain size of recrystallized specimens. Also, the Micro Vickers hardness measurement using an indentation load of 4.9N were achieved for different specimens.

3. Results and discussion

3.1. Evolution of microstructure during ECAP processing

Fig. 2, shows the microstructure of the as annealed and the ECAPed specimens. As can be seen here, the microstructure of the as- annealed specimen is characterized by relatively coarse grains containing annealing twins. The average grain size of the as annealed specimen is evaluated as about 20 µm. Imposition the first pass of ECAP causes stretching of the grains and increase of their aspect ratios, as shown in Fig. 2 (b). This effect is more evident after the second and fourth passes of the ECAP, as shown in Figs. 2 (c) and (d).

Table 1. The chemical composition of received material.

Elements	Fe	C	Cr	Ni	Mo	Cu	Mn	Co	Ti	N
Wt%	Bal.	0.02	16.47	10.39	2.09	0.36	0.81	0.21	0.01	0.04

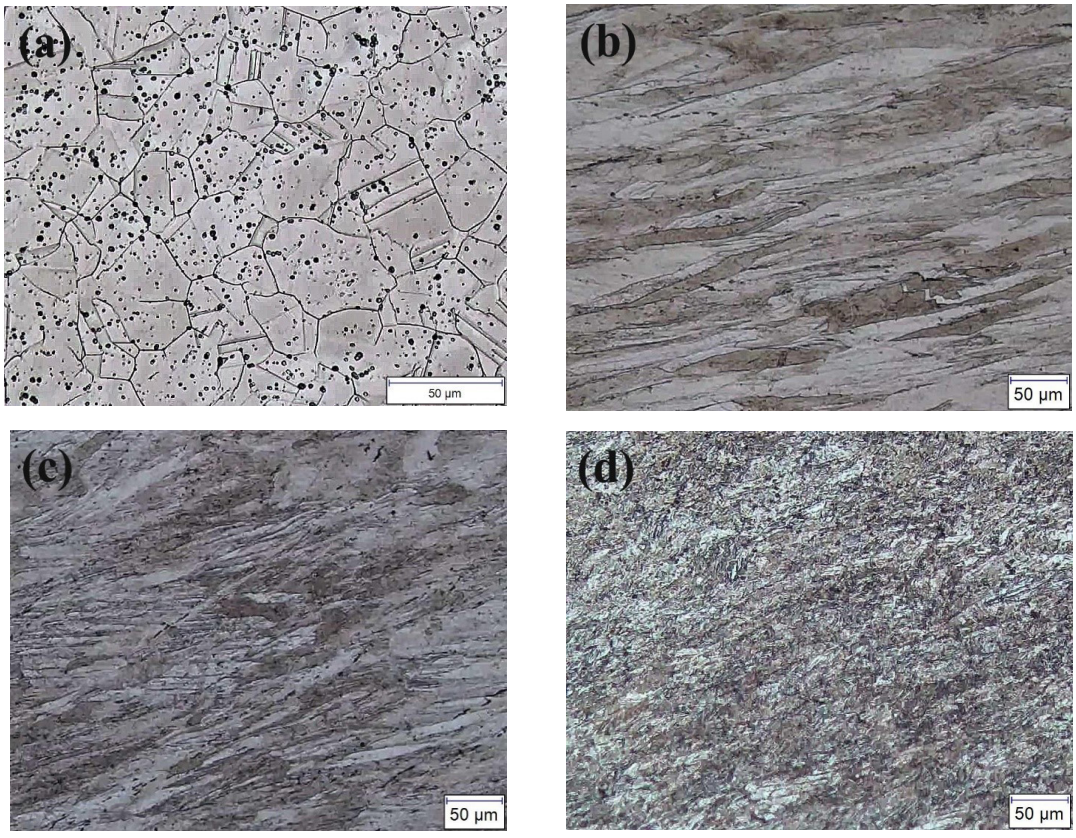

Fig. 2. OM microstructure of (a) As annealed, (b) 1pass, (C) 2 pass, and (d) 4 pass specimens. The direction of the figures is the ECAP processing direction.

3.2. Evolution of microstructure during annealing

Figs. 3, 4, and 5 show the microstructure of the ECAP processed material after exposure of 9 to 30 min. of annealing at 800 ℃. As can see here, new grains nucleate at the boundaries of the previously stretched grain during the recrystallization. This because of high stored energy in these boundaries (i.e., accumulation of dislocations, twins, etc.). The recrystallized grains grow during the time of recrystallization and therefore, the volume fraction of recrystallization (X_V) increases. According to previous studies, in metals with low stacking fault energy (SFE) like ASS, the mobility of dislocations and the recovery rate is low, and therefore, the discontinuous static recrystallization plays the predominant role during the annealing [12,16]. Comparing the microstructure evolutions of different specimens, one can trace the increase in recrystallization rate by the increase of the imposed ECAP pass number. For example, while the stretched grains of the 1 pass ECAPed specimen remain even after 30 min. of annealing, their counterpart's insides 2 and 4 passes processed specimens disappear after 15 min. of annealing. Also, the volume fraction of recrystallization for 2 and 4 passes processed specimens after 21 min. is 82% and 91% respectively and almost completed after 30 min. of annealing, while a considerable unrecrystallized region remains inside 1 pass processed specimen after a similar duration.

Fig. 6, shows the result of SEM observations of the annealed specimens. As can be seen, the results of SEM observations verify the OM observations. Also, one can see the formation of annealing twins inside the specimen's microstructures. Also, it is notable that the average size of the recrystallized grains of the specimen processed by 1, 2, and 4 passes of ECAP after 30 min. of annealing is 5.2, 4.8, and 3.3 μm, respectively.

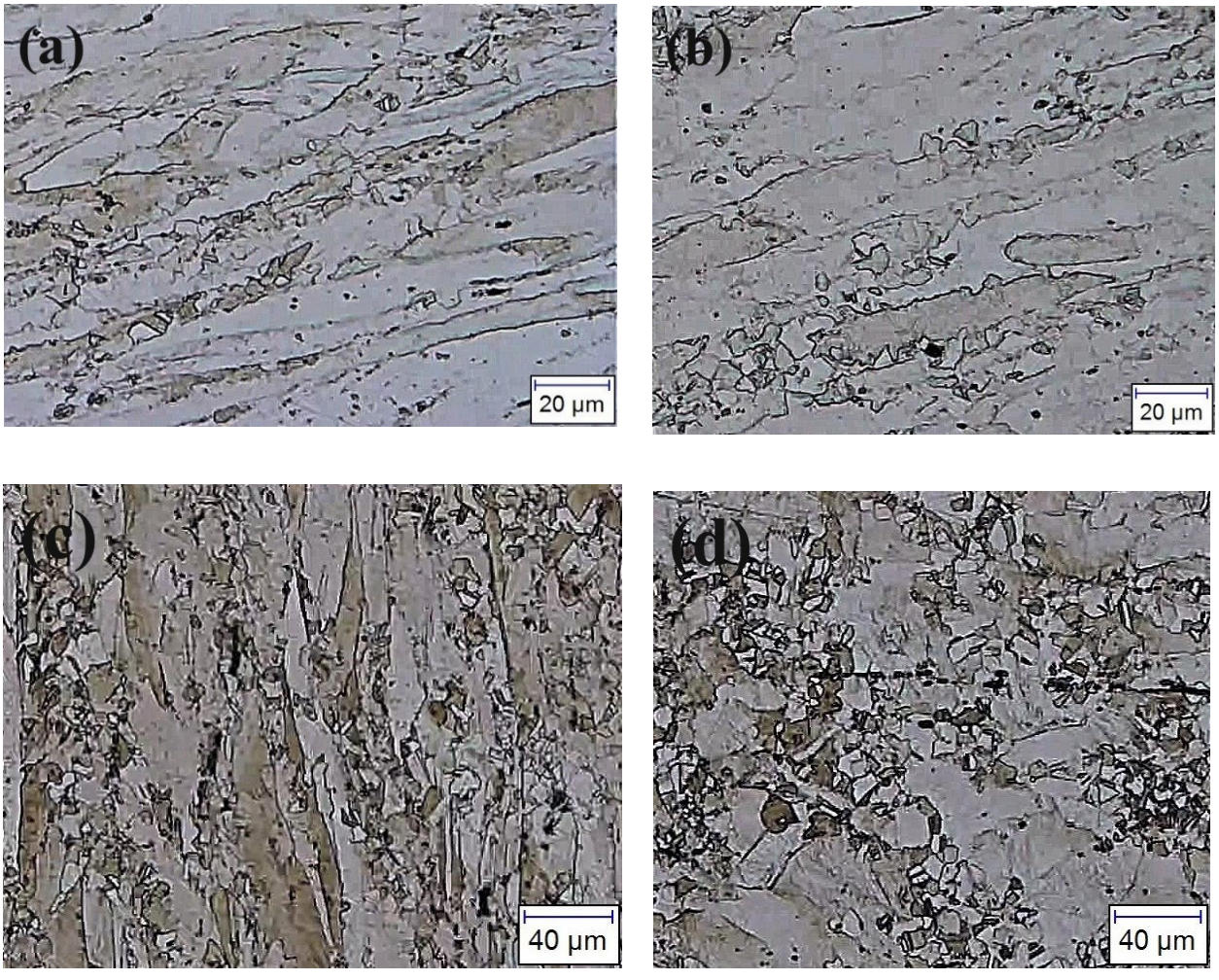

Fig. 3. OM microstructure of 1 pass specimens after annealing at 800℃ in the duration of a) 9 min, b) 15 min, and c) 30 min.

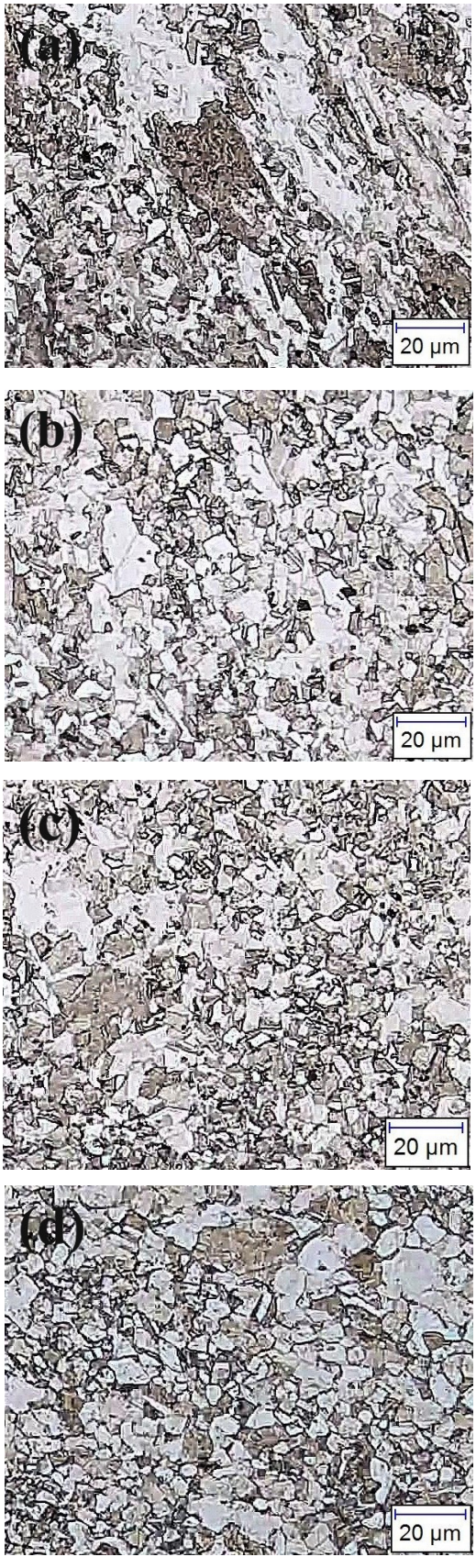

Fig.4. OM microstructure of 2 pass specimens after annealing at 800°C in the duration of a) 9 min, b) 15 min, and c) 30 min.

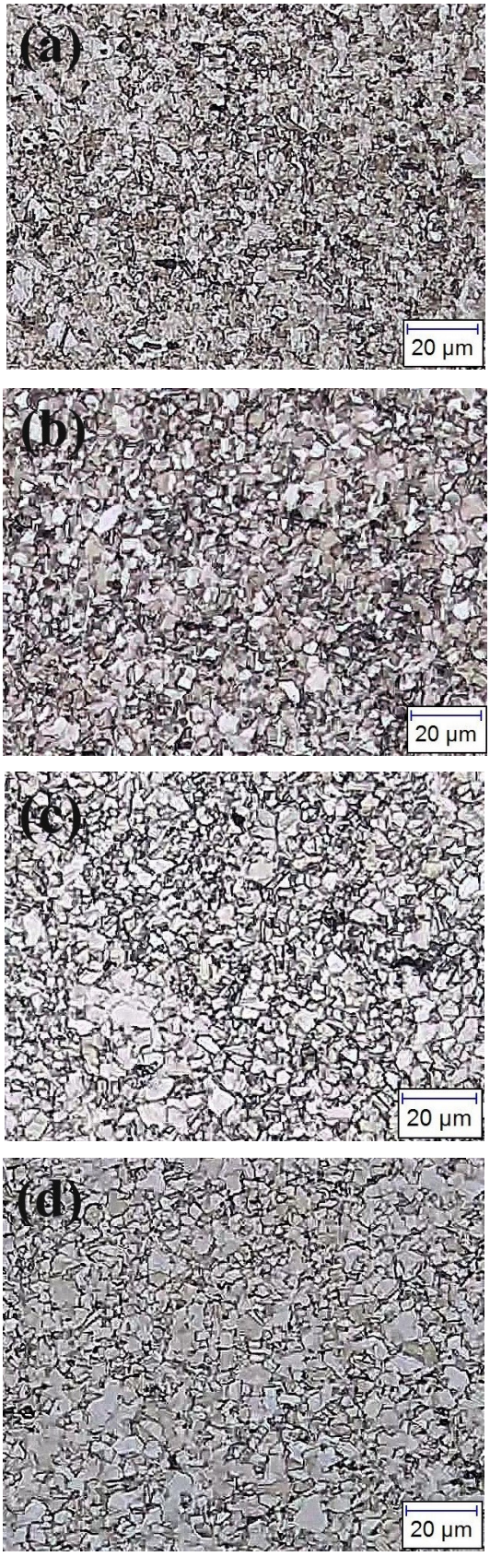

Fig.5. OM microstructure of 4 pass specimens after annealing at 800°C in the duration of a) 9 min, b) 15 min, and c) 30 min.

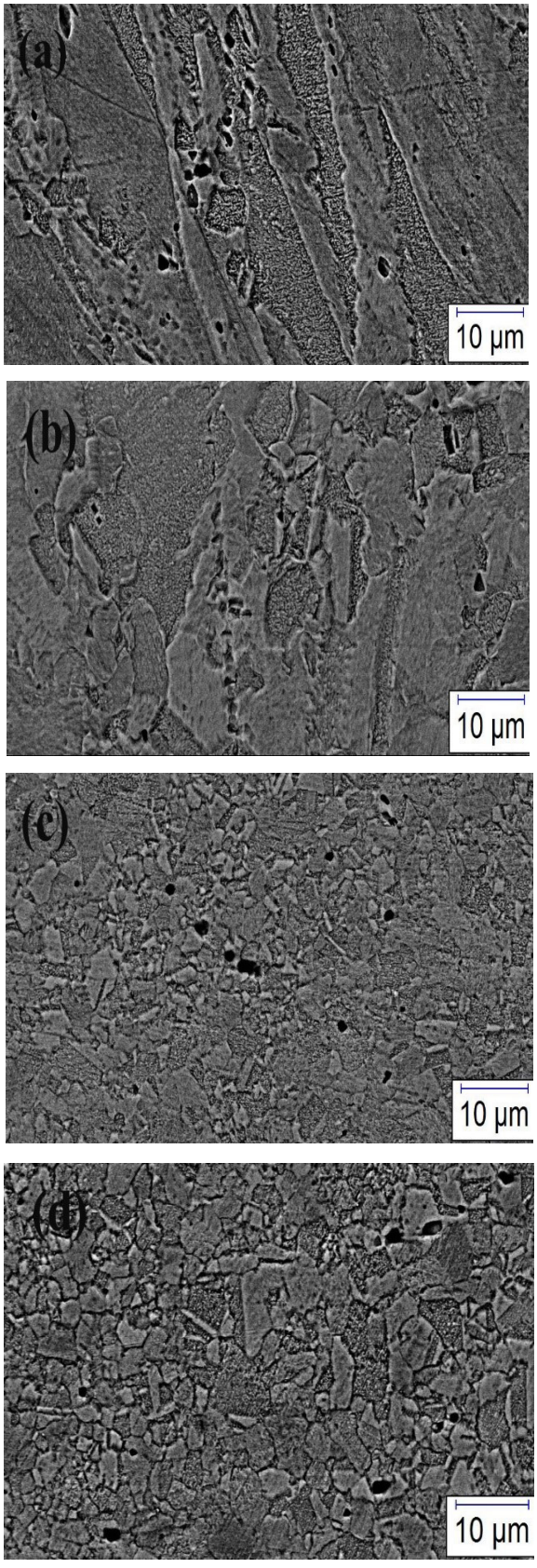

Fig. 6. SEM microstructure of the annealing specimens after: (a, c) 9 min and (b, d) 21 min. (a) and (b) are related to 1 pass specimens, (c) and (d) are related to the 4 pass specimens.

3.3. Recrystallization kinetics

Fig. 7, shows variations in the volume fraction of the recrystallization during the annealing of different specimens. As can be seen here, while the volume fraction of recrystallization slowly increases at the initiation of the annealing, the rate of recrystallization accelerates after a few minutes of annealing. The slow rate of recrystallization at the initiation of annealing is attributed to the time needed for the nucleation of new grains [14]. It is also noteworthy that the needed time for the acceleration of recrystallization decreases by increase of the ECAP pass number. Also, one can see that the recrystallization rate after the imposition of the first pass of ECAP is relatively slow compared to what is seen after the imposition of the other passes of ECAP. For more explanations, $\mathbf{t_{0.5}}$ (the time required for recrystallization of 50% of the microstructure) decreases with the increase of ECAP pass number, as can be seen in Table 2. These phenomena are attributed to the increase of the stored energy of the alloy by the increase of ECAP pass number, which accelerates the nucleation and growth of recrystallization [14].

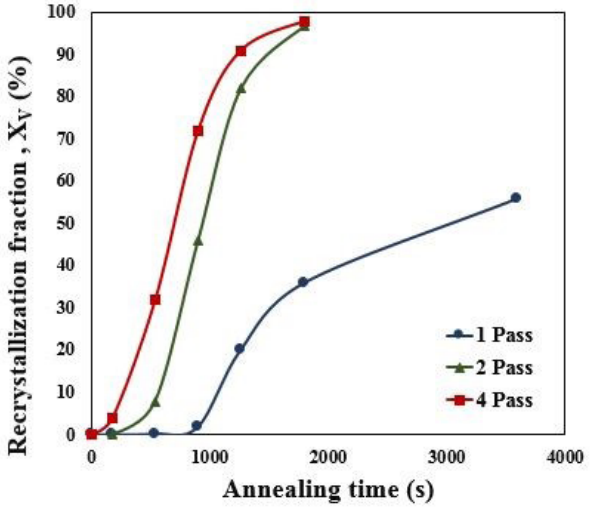

Fig. 7. Volume fraction recrystallization diagrams of annealed specimens after ECAP process.

Table 2. The recrystallization rate of specimens subjected to different passes of ECAP. These data are evaluate considering Eq. 3.

Specimens	1 pass	2pass	4pass
$\mathbf{t_{0.5}(s)}$	3000	945	700
Recrystallization rate $(*\mathbf{10^{-2}})\ (s^{-1})$	0.033	0.105	0.142

Considering Eq. 1, the JMAK model can be presented as follows:

$$Ln\left(Ln\left(\frac{1}{1-X_V}\right)\right) = nLnt + Ln\ B \qquad \text{Eq.(4)}$$

Therefore, the exponent of time (n-value) in the JMAK model can be seen as the slope of the diagram plotting $Ln(Ln\left(\frac{1}{1-X_V}\right))$ versus Lnt [15]. Fig. 8 presents the plotting of this diagram using the results of this work. As can be seen here, the n-value for all specimens is between 3 and 4. However, the n-value gradually decreases by the increase of the annealing time. For instance, one can trace that the *n-value* is near 4 at the initiation of the recrystallization. It converges to 3 at long durations of recrystallization. As mentioned in the explanations of Eq. 2, when the nucleation continues during the recrystallization time, and the growth direction is three-dimensional, the n-value would be 4. In comparison, when the growth is three-dimensional, an n-value equal to 3 means that the recrystallization continues only by the growth of existent recrystallized grains [17-19]. Regarding these explanations and considering Figs. 3 to 6 showing the three-dimensional growth of grains, one can infer that the effect of new grains nucleation on the kinetic of recrystallizations decreases during the recrystallization time, and converges to the negligible amount at long durations. Similar works have reported the decrease of n-value at a long duration of recrystallization because of a similar reason. This phenomenon is attributed to the decrease of the stored energy of the unrecrystallized regions of the materials due to the occurrence of dynamic recovery [18-20]. Also, the instability of new nuclei against the growth of previously recrystallized coarse grains could be another reason for this phenomenon [21]. It is also notable that with increasing the pass number, the *n-value* decreases more rapidly. This can be attributed to the occurrence of more rapid recovery because of the accumulation of more plastic strain energy due to the imposition of further passes of ECAP.

3.4. Vickers Hardness

Table 3 shows the variation in the Vickers hardness of the specimens during annealing. As can be seen here, the hardness of the alloy increases by the increase of the pass number of ECAP due to work- hardening. Also, while the hardness of the specimens decreases during the annealing time, the rate of hardness decrease of the one pass processed specimen is lower in comparison to other specimens. This is attributed to the relatively slow occurrence of recrystallization inside one pass processed specimens, as discussed above. Also, considering the evaluated average size of the recrystallized grains mentioned above and regarding the Hall-Petch relation of the Vickers hardness (HV) and the grain size (D) of the stainless steels 316L as below [7].

$$HV = 137.11\, D^{-0.5} + 135.13 \qquad \text{Eq.(5)}$$

One can see that the hardness of 2 and 4 passes specimens subjected to 30 min of annealing should be 197 and 210 HV, respectively. Note that these numbers are very close to the experimentally evaluated hardness of these specimens, which verifies the fulfillment of the recrystallization of these specimens similar to what is observed by OM.

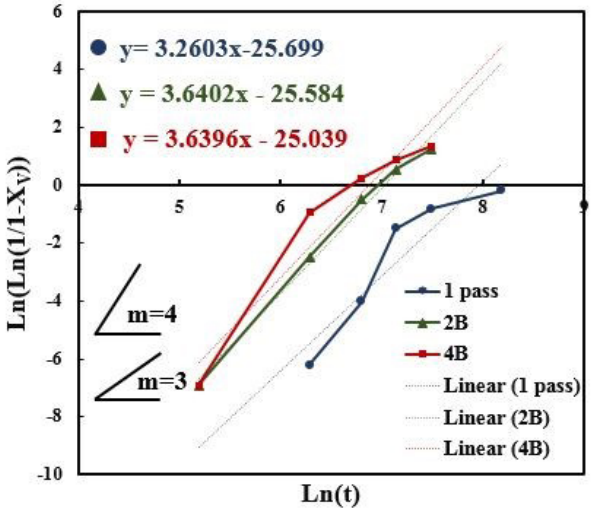

Fig. 8. JMAK diagram for the recrystallization kinetics of the ECAPed specimens.

Table 3. Vickers hardness of ECAPed and annealed specimens.

	Annealing time (min)				
specimens	0	9	15	21	30
1 pass	338	312	278	247	219
2 pass	407	292	223	212	198
4 pass	433	258	230	219	210

4. Conclusions

Considering the results of this work, it can be conclud that:

- The ASS 316L having equiaxed microstructure with a grain size less than 10μm can be obtained through processing by ECAP at 310ºC combined with subsequent annealing at 800 ºC.
- The increase of ECAP pass number accelerates the kinetics of recrystallization. For instance, the recrystallization of the alloy after the imposition of 2 and 4 passes of ECAP is almost completed after 30 min of annealing at 800 ºC.
- The *n-value* of the JMAK model at the initiation of recrystallization is close to four due to the concurrent occurrence of new grains nucleation and three-dimensional growth of these grains. However, this number converges to about three in the long duration of recrystallization due to discontinuing of the new grain's nucleation.
- The ECAP process increases the hardness of 316 stainless steel to 330-440 HV, while the annealing process reduces its hardness to 210-220 HV after 30 min. Hardness value for one pass annealed specimens is higher than other due to the relatively slow occurrence of recrystallization.

Reference

[1] R. Z. Valiev and T. G. Langdon, Principles of Equal-Channel Angular Pressing as A processing tool for grain refinement, progress in materials science: 51, (2006), 881–981. https://doi.org/10.1016/j.pmatsci.2006.02.003.

[2] I. Kim, J. Kim, D.H. Shin, Effects of grain size and pressing speed on the deformation mode of commercially pure Ti during equal channel angular pressing, Metallurgical and Materials Transactions: A. (2003), 1555–1558. https://doi.org/10.1007/s11661-003-0267-x.

[3] T.G. Langdon, M. Furukawa, M. Nemoto, Using equal-channel angular pressing for refining grain size, The Journal of The Minerals, Metals & Materials Society (TMS): 52, (2000), 30–33. https://doi.org/10.1007/s11837-000-0128-7

[4] A.F. Padilha, R. Lesley, Plaut, and P. Rangel Rios, Annealing of cold-worked austenitic stainless steels, ISIJ international: 43(2), (2003), 135-143. https://doi:10.2355/isijinternational.43.135.

[5] S.V. Dobatkin, V.F. Terent, W. Skrotzki, Structure and fatigue properties of 08Kh18N10T steel after equal-channel angular pressing and heating, Russian Metallurgy: 2012, (2012), 954–962. https://doi.org/10.1134/S0036029512110043

[6] S. V. Dobatkin, D. V. Prosvirnin, and G. I. raab, Enhanced mechanical and service properties of ultrafine grained copper-based alloys with Cr, Zr, and Hf additives, materials science: 3, no. 1 (2017), 3-5.

[7] M.J. Sohrabi, M. Naghizadeh, and H. Mirzadeh, Deformation-induced martensite in austenitic stainless steels, Archives of Civil and Mechanical Engineering: 20, (2020), 1-24. https://doi.org/10.1007/s43452-020-00130-1.

[8] Li. Jiansheng, et al. Superior strength and ductility of 316L stainless steel with heterogeneous lamella structure, Journal of Materials Science: 53.14, (2018), 10442-10456. https://doi.org/10.1007/s10853-018-2322-4.

[9] S.V. Dobatkin, W Skrotzki, and E.V. Zolotarev, Structural changes in metastable austenitic steel during equal channel angular pressing and subsequent cyclic deformation Materials Science and Engineering: A. 723, (2018), 141-147, https://doi.org/10.1016/j.msea.2018.03.018.

[10] M. Calmunger, G. Chai, R. Eriksson, et al. Characterization of Austenitic Stainless Steels Deformed at Elevated Temperature, Metall Mater Trans: A. 48, (2017), 4525–4538. https://doi.org/10.1007/s11661-017-4212-9.

[11] X. Wang, D. Wang, J. Jin, J. Li, Effects of rhenium on the microstructure and creep properties of novel nickle-based single crystal superalloys, Materials Science and Engineering: A. 761, (2019), 138042. https://doi.org/10.1016/j.msea.2019.138042.

[12] T. Sakai, A. Belyakov, R. Kaibyshev, Dynamic and post-dynamic recrystallization under hot, cold and severe plastic deformation, conditions Progress in Materials Science: 60, (2014),130-207. https://doi.org/10.1016/j.pmatsci.2013.09.002

[13] Y. H. Zhao, Y. T. Zhu, Z. Horita and T. G. Langdon, Grain growth and dislocation density evolution in a nanocrystalline Ni–Fe alloy induced by high-pressure torsion, Scripta Materialia: 64 (2011), 327–330. doi:10.1016/j.scriptamat.2010.10.027.

[14] F. J. Humphreys and M. Hatherly: Recrystallization and Related Annealing Phenomena, 1995.

[15] M. Askari Khan-abadi, M.H. Farshidi, and M.H. Moayed, Microstructure Evolution of the Stainless Steel 316L Subjected to Different Routes of Equal Channel Angular Pressing, Iranian Journal of Materials Forming: 8.2 (2021): 4-11. https://doi: 10.22099/IJMF.2021.38714.1169.

[16] D. Mandal and I. Baker, on the effect of fine second-phase particles on primary recrystallization as a function of strain, Acta materialia: 45.2 (1997): 453-461. https://doi.org/10.1016/S1359-6454(96)00215-7.

[17] A. Burbelko, E. Fraś, and W. Kapturkiewicz, About Kolmogorov's statistical theory of phase transformation, Materials Science and Engineering: A. 413, (2005), 429-434. https://doi.org/10.1016/j.msea.2005.08.161

[18] J. E. Bailey and P.B. Hirsch, The recrystallization process in some polycrystalline metals, Proceedings of the Royal Society of London. Series A. Mathematical

and Physical Sciences: 267.1328 (1962): 11-30. https://doi.org/10.1098/rspa.1962.0080.
[19] M. Oyarzábal, A. Martínez and I. Gutiérrez, Effect of stored energy and recovery on the overall recrystallization kinetics of a cold rolled low carbon steel, Materials Science and Engineering: A. 485.1-2 (2008): 200-209. https://doi.org/10.1016/j.msea.2007.07.077.
[20] A. Martınez-de-Guerenu and et al. Recovery during annealing in a cold rolled low carbon steel, Part I: Kinetics and microstructural characterization, Acta materialia: 52.12 (2004), 3657-3664. https://doi.org/10.1016/j.actamat.2004.04.019
[21] E. A. Grey and G. T. Higgins, Solute limited grain boundary migration: A rationalisation of grain growth, Acta Metallurgica: 21.4 (1973): 309-321. https://doi.org/10.1016/0001-6160(73)90186-7.